Dalton Transactions

ROYAL SOCIETY OF CHEMISTRY

PERSPECTIVE

View Article Online
View Journal | View Issue

Cite this: *Dalton Trans.*, 2025, **54**, 4396

Recent developments and challenges of molecular design in linear cyanido-bridged multimetallic complexes

Jin-Hui Fu,[a,b] Bing-Chang Tan,[a,b] Ying Song,[a,b] Zi-Hang Wu,[a,b] Xin-Tao Wu [a] and Tian-Lu Sheng *[a]

Received 30th October 2024,
Accepted 17th January 2025

DOI: 10.1039/d4dt03028a

rsc.li/dalton

Cyanido-bridged multimetallic complexes have been extensively studied for their potential applications in molecular electronics and spintronics. The design of these complexes involves the strategic placement of metal centers and the use of cyanide bridges to facilitate electron transfer between metal ions. The challenges in this field include the precise control of the electronic states and the stability of the complexes under various conditions. Researchers are exploring new synthetic methods and functionalization strategies to overcome these challenges and to enhance the performance of these complexes in practical applications. Overall, this review demonstrates the design of linear cyanido-bridged multimetallic complexes and related electronic properties, emphasizing the remaining challenges.

1. Introduction

Molecule-based materials derived from cyanido-bridged multimetallic complexes have been widely developed due to their interesting electronic, photophysical and magnetic properties.[1–7] Cyanido-bridged mixed-valence systems, which involve organometallics linked by cyanide, play a significant role in the study of electron transfer and magnetism.[8,9] Cyanido-bridged multimetallic complexes derive their properties from the asymmetric binding capability of the cyanide group. This unique characteristic enables precise design of molecular length and shape. Furthermore, their molecular structures and electronic properties can be systematically tailored. By fine-tuning the composition, arrangement, and interactions within these complexes, researchers can explore a vast array of potential material properties and applications, pushing the boundaries of what is achievable in the field of electric and magnetic materials science.

In the past decades, a large number of cyanido-bridged mixed-valence complexes with different molecular shapes and lengths have been reported by Vogler,[10] Haim,[11] Scandola,[12] Bocarsly,[13] Meyer,[14] Denning,[15] Connelly,[16] Endicott,[17] Vahrenkamp[7] and Baraldo[1] *et al*. The research focus has gradually shifted from the initial structural composition to electronic coupling between metals.

The intramolecular electron transfer process in cyanido-bridged mixed-valence systems is influenced by a series of factors: (i) the nature of metal ions; (ii) the auxiliary ligands on metals; (iii) the distance between interacting metal centers; (iv) the shape of the molecule; (v) the orientation of the cyanide bridges; (vi) the solvent polarity. There has been a significant effort towards the search for appropriate fragments that can be used to synthesize fully delocalized Robin–Day[18] Class III cyanido-bridged mixed-valence complexes. The Class III cyanido-bridged mixed-valence system was first prepared by regulating the energy between construct blocks by Baraldo *et al.* in 2014.[19,20] Since then, Sheng *et al.* reported another fully delocalized trinuclear cyanido-bridged mixed-valence species with complete crystallographic characterization.[21] Despite the fact that these delocalized cyanido-bridged mixed-valence systems are fascinating because of their unique crystallographic and physical properties, it is still a challenge to synthesize delocalized cyanido-bridged molecular rods with higher nuclearities.

Apart from fundamental electron transfer properties, some cyanido-bridged multimetallic complexes exhibit properties related to the electron spin state. For example, a unique linear cyanido-bridged multimetallic complex, $[Ru_2(\mu\text{-ap})_4\text{–CN–}Ru_2(\mu\text{-ap})_4][BPh_4]$ (ap = 2-anilinopyridinate), has been synthesized with uncommon electronic structures.[22] This complex features a Ru2 (S = 1/2)–CN–Ru2 (S = 3/2) configuration based on an asymmetric cyanide unit, allowing for metal-to-metal charge transfer (MMCT) between two identical Ru2 clusters that possess the same valence state but distinct spin states.[22] Recently, several linear cyanido-bridged multimetallic mole-

[a]*State Key Laboratory of Structural Chemistry, Fujian Institute of Research on the Structure of Matter, Chinese Academy of Science, Fuzhou, Fujian 350002, PR China. E-mail: tsheng@fjirsm.ac.cn*
[b]*School of Chemical Sciences, University of Chinese Academy of Sciences, Beijing 100049, PR China*

cules have demonstrated intriguing mixed spin states,[23] electron-transfer-coupled spin transition (ETCST),[24–26] spin crossover (SCO) phenomena[27] and water oxidation capabilities.[28,29] Thus, linear cyanido-bridged multimetallic complexes are not only ideal models for investigating electron transfer but also represent novel functional molecules, leveraging their controllable electronic structures and electron transfer properties. Additionally, their ability to undergo controlled spin transitions and electron transfers makes them attractive for use in sensors, where they can detect changes in environmental conditions with high sensitivity and accuracy. This versatility underscores the importance of further exploring and understanding the properties of these cyanido-bridged multimetallic molecules.

Several review articles have summarized the formation and properties of cyanido-bridged multimetallic complexes.[4,6,7,30–32] In this review, our objective is not to recapitulate the cyanido-bridged complexes that have been systematically reviewed previously, but rather to concentrate on the linear oligonuclear cyanido-bridged multimetallic complexes from the past thirty years, which primarily involve electron transfer properties and electron structures. We also emphasize the challenges associated with molecular design using various transition metal fragments.

2. Linear cyanido-bridged multimetallic complexes

To date, a substantial number of cyanido-bridged complexes have been reported for the study of electron transfer, magnetism, and spin-crossover (SCO) behavior, among other properties. In this section, we will discuss and summarize the recent progress of linear cyanido-bridged complexes including molecular design, electron transfer, SCO behavior and some uncommon electron structures.

2.1 Molecular design

The basic strategy of molecular design of dinuclear and trinuclear species has been summarized in the literature.[7] To date, the construction of linear molecules with high nuclearities such as tetranuclear and pentanuclear complexes remains a major challenge because of difficulties in separation and synthesis. The intricate nature of their structure and the complexity involved in their formation pose substantial obstacles. The dinuclear and trinuclear complexes with one or two open coordination sites on the *para*-side are useful precursors (Fig. 1). In this case, the challenge is controlling the length of the linear chain and the solubility of chain-like complexes.

More recently, Baraldo and coworkers have reported a series of linear cyanido-bridged heptanuclear complexes using trinuclear building blocks (Fig. 2a),[33] which is a good synthetic route. However, since then only one case of linear pentanuclear cyanido-bridged molecules with an Fe-NC-Ru-NC-Ag-CN-Ru-CN-Fe core has been reported by the oxidation of trinuclear species with excess $AgBF_4$ (Fig. 2b).[34] Unfortunately, the reaction mechanism is not clear. To date, finding appropriate building units to synthesize molecules with ideal nuclei remains difficult. In our opinion, an excellent construction block needs good electronic mediating ability and controllable reaction conditions. Sheng *et al.* reported two dinuclear complexes of the type M_A-CN-M_B-L, where the *para*-substituted ligand L can be substituted by M-CN by controlling the proportion of reactants and temperature, which may be a family of excellent construction units because of their Class II–III electronic delocalization characteristics after one-electron oxidation.[35] In addition, some metal clusters such as $Ru_2(DMBA)_4$,[36–38] $Ru2(OAc)_4$,[39] $[Co_3(dpa)_4]^{2+}$ (ref. 39) and $[Ni_5(tdpa)_4]^{2+}$ (ref. 39) were also used for constructing linear tetra- (Fig. 3a), penta- (Fig. 3b) and heptanuclear complexes

Fig. 1 Schematic diagram of precursor compounds with open coordination sites (L = *para*-substituted ligand).

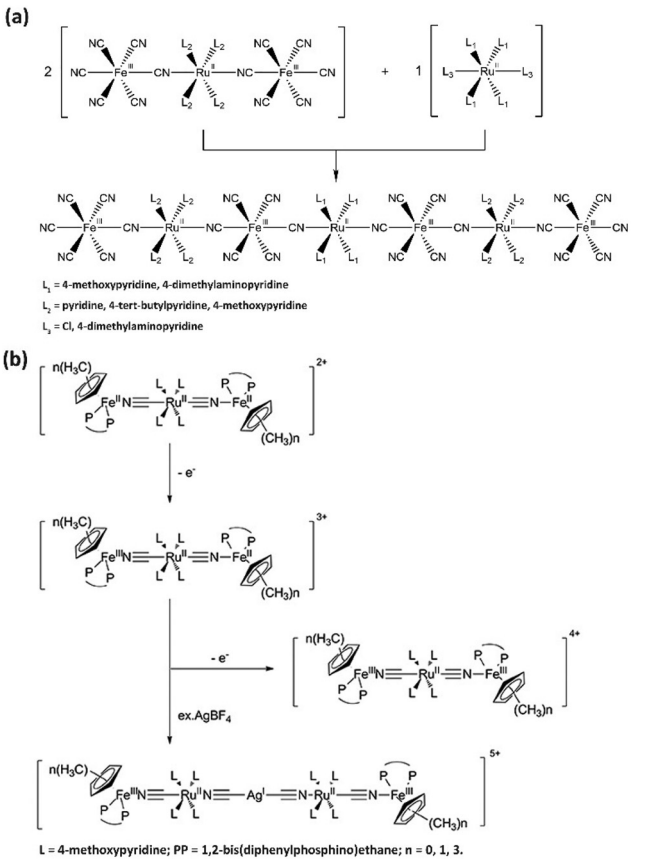

Fig. 2 The synthetic route of linear molecules: (a) heptanuclear complexes and (b) pentanuclear complexes. Adapted with permission from ref. 34. Copyright 2023 Wiley-VCH.

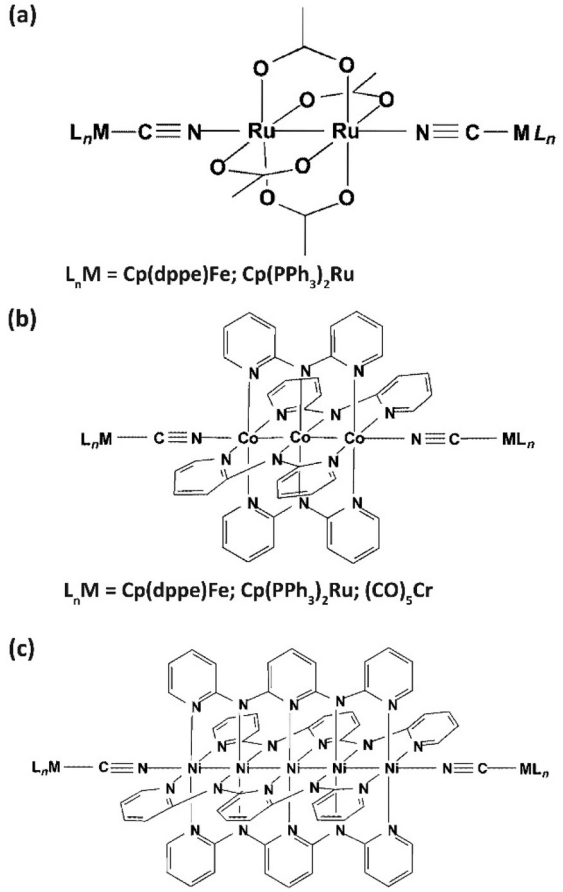

Fig. 3 The molecular diagram of linear tetra- (a), penta- (b) and hepta-nuclear (c) complexes with metal clusters. Adapted with permission from ref. 39. Copyright 2003 Wiley-VCH.

(Fig. 3c). These metal clusters may also serve as potential building blocks for further development. Each attempt brings about new insights and understanding, but the ultimate goal of achieving stable, high-nuclearity linear molecules remains an ongoing endeavor.

2.2 Electronic properties

2.2.1 Metal-to-metal charge transfer. Metal-to-metal charge transfer (MMCT) in cyanido-bridged mixed-valence (MV) complexes is a major research topic in this field. As the greatest ones, dinuclear cyanido-bridged complexes (M-CN-M′) represent the simplest cyanido-bridged MV systems for the investigation of intramolecular MMCT properties. A series of homobinuclear and heterobinuclear cyanide-bridged MV complexes have been researched by Haim,[11] Vogler,[40] Scandola,[41] Vahrenkamp,[42,43] Baraldo[1,44–46] and Sheng[35,47–52] *et al*. Among the reported dinuclear MV systems, a family of Ru-CN-Ru complexes $[Ru^{II}(tpy)(bpy)(\mu\text{-}CN)Ru^{II}(py)_4L]^{3/4+}$ and $[Ru^{II}(tpy)(bpy)(\mu\text{-}CN)Ru^{II}(bpy)_2L]^{3/4+}$ (L = Cl^-, NCS^-, DMAP, and ACN; tpy = 2,2′,6′,2″-terpyridine; bpy = 2,2′-bipyridine; py = pyridine; DMAP = 4-dimethylaminopyridine; ACN = acetonitrile) are typical examples (Fig. 4).[44,45] The electrochemical splitting of

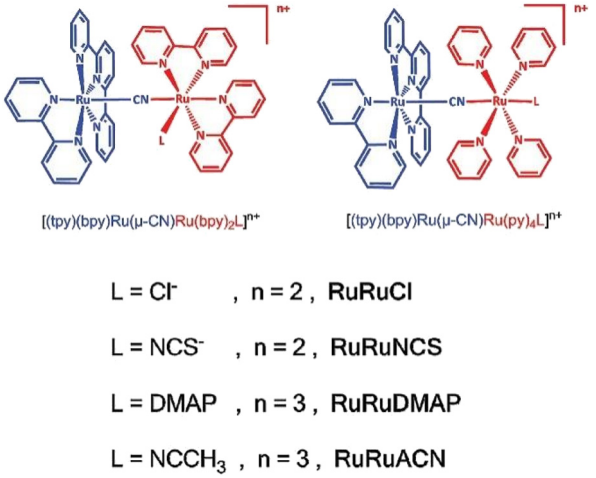

Fig. 4 The diagram of dinuclear complexes RuRuL. Adapted with permission from ref. 44. Copyright 2020 Royal Society of Chemistry.

the two Ru centres decreases as the ligand L varies from Cl^- to ACN, and the corresponding MMCT absorption bands also exhibit greater intensity and lower energy, indicating stronger electron coupling. For electron coupling between two metal centers, the key lies in the modulation of the redox potentials of the metal centers, which can be fine-tuned by altering the ligand field strength. For instance, by choosing ligands that stabilize higher oxidation states, one can create systems that favor electron donation.

Conversely, ligands that stabilize lower oxidation states can be used to design systems that are more receptive to electron acceptance. Furthermore, the complex $[Ru^{II}(tpy)(bpy)(\mu\text{-}CN)Ru^{II}(py)_4L]^{4/5+}$ exhibited a stronger electronic coupling compared to $[Ru^{II}(tpy)(bpy)(\mu\text{-}CN)Ru^{II}(bpy)_2L]^{4/5+}$, which indicates that the ligand L positioned at the *para*-position of CN is beneficial for electron coupling. This suggests that there are different degrees of orbital overlap in the *trans*- and *cis*-configurations. Based on the systematic study, a fully delocalized (Robin–Day Class III) MV complex $[Cp^*(dppe)Ru^{II}(\mu\text{-}CN)Ru^{III}(bpy)_2Cl]^{2+}$ (Cp* = 1,2,3,4,5-pnetamethylcyalopentaiene; dppe = 1,2-bis(diphenylphosphino)ethane) has been structurally characterized (Fig. 5).[49] By alternating the highly deloca-

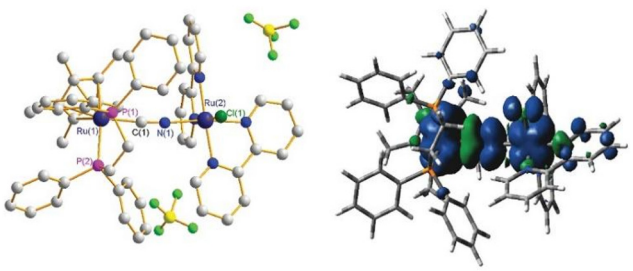

Fig. 5 The single-crystal structure and computed spin densities of the fully delocalized dinuclear cyanido-bridged complex. Adapted with permission from ref. 49. Copyright 2022 Royal Society of Chemistry.

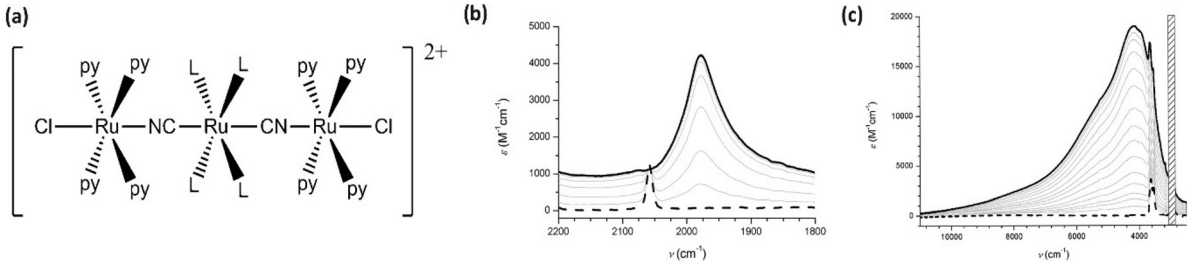

Fig. 6 (a) The structure diagram of the first fully delocalized species. (b) IR spectra. (c) Vis-NIR absorption spectra. Adapted with permission from ref. 19. Copyright 2014 Wiley-VCH.

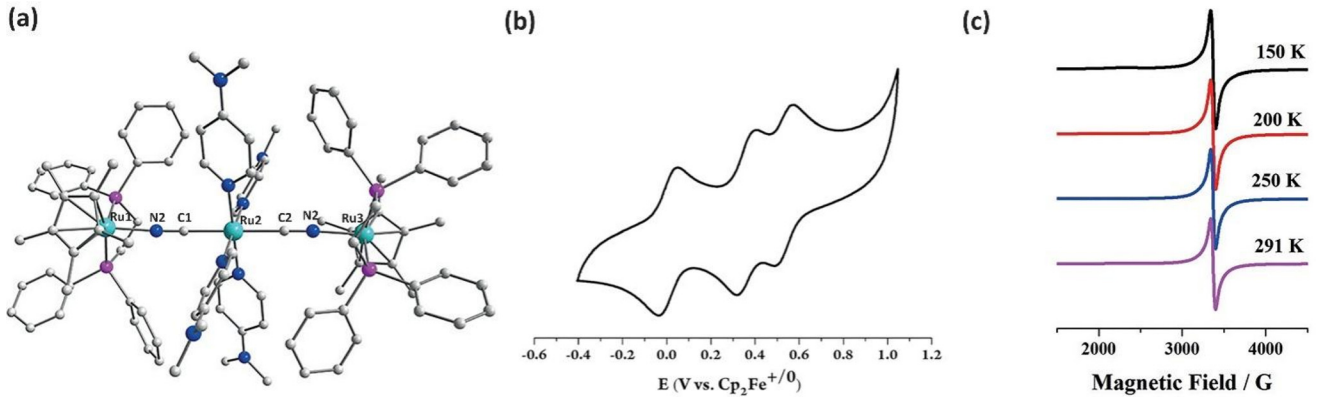

Fig. 7 (a) The molecular structure of *trans*-[Cp*(dppe)Ru(μ-NC)Ru(dmap)$_4$(μ-CN)Ru(dppe)Cp*]$^{3+}$. (b) Cyclic voltammogram in CH_2Cl_2. (c) The variable temperature EPR spectra. Adapted with permission from ref. 21. Copyright 2018 Wiley-VCH.

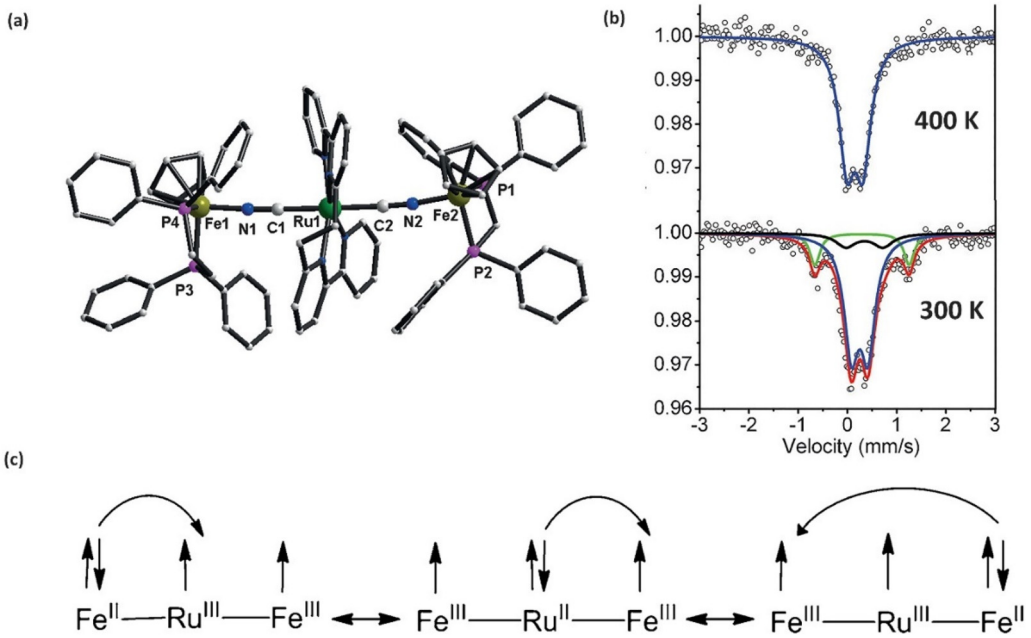

Fig. 8 (a) The molecular structure of *trans*-[Cp(dppe)Fe(μ-NC)Ru(o-bpy)(μ-CN)Fe(dppe)Cp][PF_6]$_4$. (b) Variable temperature Mössbauer spectra. (c) The description of thermally induced electron delocalization. Adapted with permission from ref. 68. Copyright 2017 Wiley-VCH.

lized dinuclear block, penta- or hepta-nuclear species with excellent remote electronic communication may become a reality, heralding a promising future in this field.

For trinuclear cyanido-bridged systems, the MMCT is complicated but interesting due to more metal centers and isomers (cyanide or isocyanide and *trans* or *cis*). The long-range electron communication, a crucial aspect in chemical, physical, and biological systems, stands as a priority research focus within trinuclear systems. Meyer,[14] Scandola[12,41] and Vahrenkamp[53–58] *et al.* have conducted a large number of foundational research studies. However, most of the reported trinuclear cyanido-bridged MV complexes belong to the Class II system. Recently, the first fully delocalized trinuclear cyanido-bridged complex has been reported.[19] The guiding principle for the design and synthesis of this complex lies in the energy regulation among its components. As depicted in Fig. 6, the complex exhibits only a broad cyanide stretching absorption band, indicating a symmetrical ground state. The NIR spectrum exhibits a narrow and intense absorption band characterized by a "cutoff" profile. Likewise, Sheng *et al.* reported the first example of a structurally characterized trinuclear cyanido-bridged complex *trans*-[Cp*(dppe)Ru(μ-NC)Ru(dmap)$_4$(μ-CN)Ru(dppe)Cp*]$^{3+}$ (Fig. 7), completing the structural features of delocalized cyanido-bridged systems.[21] More recently, a family of linear cyanido-bridged and isocyanido-bridged trinuclear systems with fine ligand substitution have been investigated using [Cp(Me)$_n$(dppe)M] (n = 0, 1, 3, 4, 5; M = Ru, Fe) fragments, where the transition from Robin–Day Class II to Class III has been implemented in these systems.[59–67] The study of these delocalization systems can continuously refine the theoretical model, enhancing its ability to more accurately predict the behavior of the delocalized molecules under various conditions. Apart from that, the first thermally induced Class III cyanido-bridged MV complex *trans*-[Cp(dppe)Fe(μ-NC)Ru(o-bpy)(μ-CN)Fe(dppe)Cp][PF$_6$]$_4$ (Fig. 8)[68] provides the possibility for further designing functional cyanido-bridge molecules. In this instance, the IR and EPR spectra deviate from those of a similar valence-localized complex. The magnetic data and Mössbauer spectra reveal a thermally induced delocalized mode (Fig. 8c).

Although dinuclear and trinuclear systems have been extensively studied, linear cyanido-bridged multimetallic complexes with higher nuclearities where the cyanide as a bridge links every two metal centers are still rare. A lot of high nuclear cyanido-bridged complexes adopt a non-linear configuration such as zigzag,[69] square,[70] and cubic.[71] The first example is a family of linear heptanuclear species (Fig. 2a).[33] Electrochemical measurements indicate the presence of long-range electronic coupling between the two terminal iron (Fe) centers in the complex *trans*-[L$_4$Ru^{II}{(μ-NC)Fe^{III}(NC)$_4$(μ-CN)Ru^{II}(MeO-py)$_4$(μ-NC)Fe^{III}(CN)$_5$}$_2$]$^{6-}$, although the fact is that these terminal Fe atoms are separated by a distance of 3 nm. The implications of this finding could pave the way for novel applications in fields such as molecular electronics, where effective long-range electronic communication is crucial. Additional studies are needed to further elucidate the mechanisms underlying this remarkable phenomenon and explore its potential for practical utilization.

A few linear cyanido-bridged systems linking di-, tri- and penta-metal clusters have been developed by Vahrenkamp and Sheng *et al.* (Fig. 3). However, the long-range electron coupling between the two terminal blocks is not observed because of the poor electronic properties of these cores. The research topic for these complexes is mainly limited to electronic communication between adjacent cores. For example, a series of tri-, tetra- and penta-nuclear MV systems with Ru2 cores were systematically investigated by Sheng *et al.*[22,36–38,72–75] Moreover, the results suggest the existence of long-range electronic communication in the Fe–CN–Ru2–NC–Fe series.

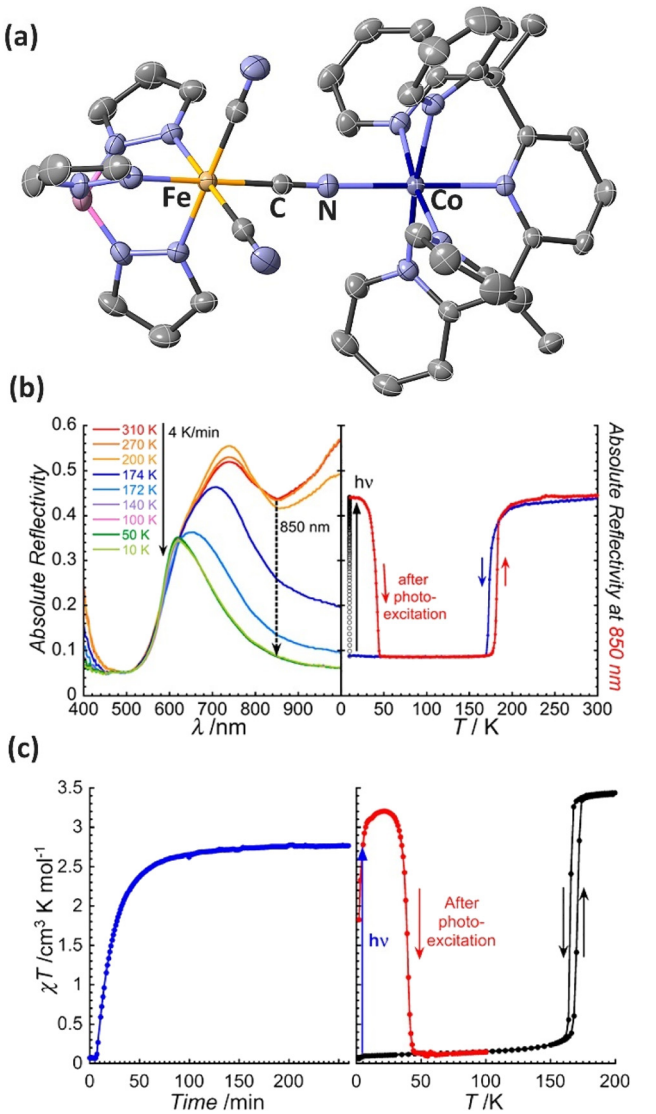

Fig. 9 (a) Structure of [Fe(tp)(CN)$_3$][Co(Py$_5$Me$_2$)]$^+$. (b) Surface reflectivity from 300 K to 10 K and absolute reflectivity at 850 nm. (c) χT *versus* time at 1 T under white-light irradiation at 10 K and χT *versus* temperature plots. Adapted with permission from ref. 24. Copyright 2014 American Chemical Society.

In addition to the studies of electron transfer, the properties related to the electron transfer process have also been reported such as electron-transfer-coupled spin transition (ETCST). For example, dinuclear complexes $[Fe(tp)(CN)_3][Co(Py_5Me_2)][OTf]$[24,25] (Fig. 9) and $[Fe(H_2bimpy)(CN)_3][Co(Py_5Me_2)]\cdot 2.5CH_3OH$ [26] exhibit significant variation in electronic and magnetic properties caused by MMCT. Similarly, other linear cyanido-bridged systems with ETCST properties have also been reported.[76]

To date, the majority of ETCST cyanido-bridged multimetallic complexes feature non-linear structures, and we will not discuss them here.

2.2.2 Spin-crossover. Complexes containing a first row d^4–d^7 transition metal can exist in high-spin (HS) and low-spin (LS) states, which is decided by the ligand field strength. Thus, complexes with a medium ligand field strength can switch between HS and LS states under external stimulation such as heat, pressure and light, which is called spin-crossover (SCO) behavior. Cyanido-bridged multimetallic complexes with the SCO phenomenon have a long history, starting from Prussian blue analogues. For linear oligonuclear cyanido-bridged systems, their SCO behaviors are more easily regulated and utilized, especially in the regulation of spin transition temperature.

Recently, Tao Liu and coworkers reported a series of linear cyanido-bridged SCO complexes with an Fe-CN-Fe-NC-Fe array, where the central Fe^{II} ion in all three complexes exhibits thermal and light-induced SCO phenomena.[27]

Another example is a series of di- and tri-nuclear complexes with one or two control units reported by Sheng *et al.* (Fig. 10).[77,78] The investigation reveals that spin transition can be regulated by the electron-donating ability of the C-bond metal of cyanide, where the spin transition temperature decreases with a stronger electron-donating ability. In addition, the dinuclear species $[Py_5OMeFeNCFe(dppe)CpMe_3][OTf]\cdot CH_3CN$ exhibits a thermally induced ultrafast high-to-low spin interconversion, offering a promising prospect for the design of switchable molecules.

2.2.3 Some uncommon spin states. Two asymmetric coordination atoms of cyanide, where the carbon atom is a strong σ donor and π acceptor and the nitrogen acts as a medium σ donor, can reflect the electronic structures of the bonding metal. Herein, two linear complexes with a special spin state are reported by Sheng *et al.*[22,23] For example, the

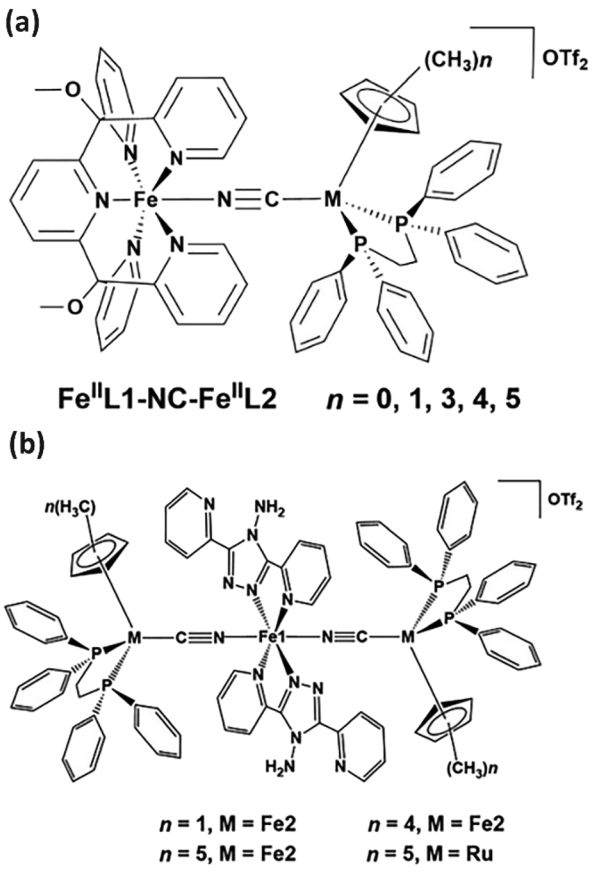

Fig. 10 (a) Molecular diagram of linear dinuclear complexes. Adapted with permission from ref. 78. Copyright 2024 American Chemical Society. (b) Molecular diagram of trinuclear SCO complexes. Adapted with permission from ref. 77. Copyright 2024 Royal Society of Chemistry.

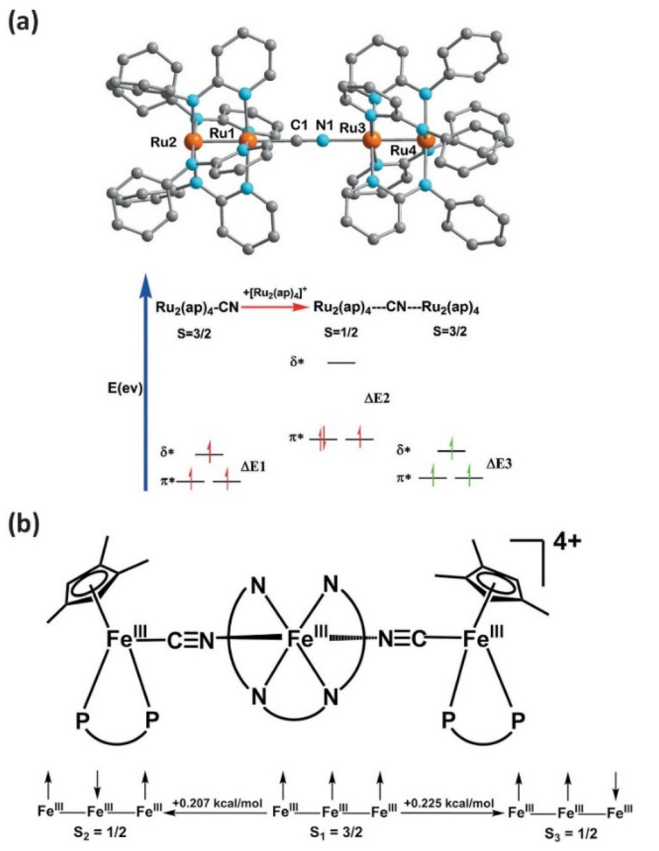

Fig. 11 (a) The structural diagram of the linear tetranuclear species and its diagram of spin states. Adapted with permission from ref. 22. Copyright 2019 Wiley-VCH. (b) The structural and spin diagram of three spin states. Adapted with permission from ref. 23. Copyright 2023 Wiley-VCH.

linear tetranuclear cyanido-bridged complex $[Ru_2(\mu\text{-ap})_4\text{–CN–}Ru_2(\mu\text{-ap})_4][BPh_4]$ (Fig. 11a) shows uncommon electron spin states.[22] The Ru_2 unit with carbon binding of cyanide has S = 1/2, while the Ru_2 unit with nitrogen binding of cyanide has S = 3/2, confirmed by the crystallographic data, magnetic measurement, IR, EPR, and theoretical calculations. Even more interesting is that a new MMCT absorption band appears between two metal centers in the same valence states. Furthermore, the preparation of this complex involved careful manipulation of the asymmetric cyanide unit, which plays a crucial role in facilitating the MMCT process. The resulting structure exhibits intriguing electronic properties due to the interplay between the different spin states of the Ru2 clusters. This multimetallic complex represents a significant advancement in the field of cyanide-bridged metal clusters and holds promise for further exploration of its potential applications in various domains, such as catalysis, materials science, and electronics. Another example is the coexistence of three spin states in the linear trinuclear Fe-CN-Fe-NC-Fe complex (Fig. 11b).[23] This unique arrangement of spin states enables the complex to exhibit intriguing magnetic properties. These uncommon electronic structures provide a new perspective for designing new molecular materials.

3. Conclusions

In summary, most of the linear cyanido-bridged multimetallic complexes reviewed here have excellent molecular electronic properties. Their structure and electronic properties can be manipulated through the selection of specific building blocks and exposure to external stimuli. As the cyanide acts as a linear and asymmetric bridging ligand, the molecular length and structures are predictable and designed. Likewise, the key parameters of functional complexes, such as electronic delocalization, spin state and redox potentials, are regulable by selecting suitable blocks. Thus, cyanide-bridged multimetallic molecules, as candidates for molecular devices, are valued not only for their designable molecular structures but also for their adjustable electronic properties.

However, some future challenges still exist. The next target in molecular designing is constructing highly delocalized complexes with higher nuclearities to further explore the remote electron transfer. For example, the design of heptanuclear molecules introduced in this article is a knocking brick. In our opinion, the degrees of electron enrichment in the middle skeleton are the foundation of long-range electronic communication. On the other hand, fully delocalized Class III cyanido-bridged MV complexes are still rare. Design and synthesis of more Class III cyanido-bridged systems to investigate their delocalized mechanism is also a continuous challenge. In addition, tuning electronic properties such as electron transfer and electron spin through external stimuli to synthesize functional molecules can be used in future molecular devices. As the molecular assembly with cyanido-bridging blocks offers high designability in chemical and physical parameters, the linear cyanido-bridged multimetallic systems described above may be promising systems for the next generations of functional molecular materials.

Data availability

The authors confirm that the data presented in the article are available and the referenced charts are authorized.

Conflicts of interest

There are no conflicts to declare.

Acknowledgements

We are grateful for the financial support from the National Natural Science Foundation of China (92261116 and 22473109).

References

1 L. M. Baraldo, P. Forlano, A. R. Parise, L. D. Slep and J. A. Olabe, *Coord. Chem. Rev.*, 2001, **219**, 881–921.
2 D. M. D'Alessandro and F. R. Keene, *Chem. Rev.*, 2006, **106**, 2270–2298.
3 Y.-S. Meng, O. Sato and T. Liu, *Angew. Chem., Int. Ed.*, 2018, **57**, 12216–12226.
4 G. N. Newton, M. Nihei and H. Oshio, *Eur. J. Inorg. Chem.*, 2011, **20**, 3031–3042.
5 M. B. Robin, *Inorg. Chem.*, 1962, **1**, 337–342.
6 S. Tanase and J. Reedijk, *Coord. Chem. Rev.*, 2006, **250**, 2501–2510.
7 H. Vahrenkamp, A. Geiss and G. N. Richardson, *J. Chem. Soc., Dalton Trans.*, 1997, 3643–3651.
8 J.-P. Launay, *Eur. J. Inorg. Chem.*, 2020, **2020**, 329–341.
9 S.-I. Ohkoshi, A. Namai and H. Tokoro, *Coord. Chem. Rev.*, 2019, **380**, 572–583.
10 A. Vogler, A. H. Osman and H. Kunkely, *Coord. Chem. Rev.*, 1985, **64**, 159–173.
11 A. Burewicz and A. Haim, *Inorg. Chem.*, 1988, **27**, 1611–1614.
12 F. Scandola, R. Argazzi, C. A. Bignozzi, C. Chiorboli, M. T. Indelli and M. A. Rampi, *Coord. Chem. Rev.*, 1993, **125**, 283–292.
13 Y. Wu, B. W. Pfennig, S. L. Sharp, D. R. Ludwig, C. J. Warren, E. P. Vicenzi and A. B. Bocarsly, *Coord. Chem. Rev.*, 1997, **159**, 245–255.
14 B. J. Coe, T. J. Meyer and P. S. White, *Inorg. Chem.*, 1995, **34**, 3600–3609.
15 W. M. Laidlaw, R. G. Denning, D. M. Murphy and J. C. Green, *Dalton Trans.*, 2008, 6257–6264.

16 G. A. Carriedo, N. G. Connelly, M. C. Crespo, I. C. Quarmby, V. Riera and G. H. Worth, *J. Chem. Soc., Dalton Trans.*, 1991, 315–323.
17 J. F. Endicott and Y.-J. Chen, *Coord. Chem. Rev.*, 2013, **257**, 1676–1698.
18 M. B. Robin and P. Day, *Adv. Inorg. Chem. Radiochem.*, 1967, **9**, 247–422.
19 G. E. Pieslinger, P. Alborés, L. D. Slep and L. M. Baraldo, *Angew. Chem., Int. Ed.*, 2014, **53**, 1293–1296.
20 G. E. Pieslinger, P. Albores, L. D. Slep, B. J. Coe, C. J. Timpson and L. M. Baraldo, *Inorg. Chem.*, 2013, **52**, 2906–2917.
21 Y.-Y. Yang, X.-Q. Zhu, S.-M. Hu, S.-D. Su, L.-T. Zhang, Y.-H. Wen, X.-T. Wu and T.-L. Sheng, *Angew. Chem., Int. Ed.*, 2018, **57**, 14046–14050.
22 S.-D. Su, X.-Q. Zhu, Y.-H. Wen, L.-T. Zhang, Y.-Y. Yang, C.-S. Lin, X.-T. Wu and T.-L. Sheng, *Angew. Chem., Int. Ed.*, 2019, **58**, 15344–15348.
23 Y. He, Y. Y. Huang, X. Q. Zhu, J. H. Fu, X. T. Wu and T. L. Sheng, *Chem. – Eur. J.*, 2023, **29**, e202300100.
24 S. F. Jafri, E. S. Koumousi, M.-A. Arrio, A. Juhin, D. Mitcov, M. Rouzieres, P. Dechambenoit, D. Li, E. Otero, F. Wilhelm, A. Rogalev, L. Joly, J.-P. Kappler, C. C. D. Moulin, C. Mathoniere, R. Clerac and P. Sainctavit, *J. Am. Chem. Soc.*, 2019, **141**, 3470–3479.
25 E. S. Koumousi, I.-R. Jeon, Q. Gao, P. Dechambenoit, D. N. Woodruff, P. Merzeau, L. Buisson, X. Jia, D. Li, F. Volatron, C. Mathoniere and R. Clerac, *J. Am. Chem. Soc.*, 2014, **136**, 15461–15464.
26 I.-R. Jeon, S. Calancea, A. Panja, D. M. P. Cruz, E. S. Koumousi, P. Dechambenoit, C. Coulon, A. Wattiaux, P. Rosa, C. Mathoniere and R. Clerac, *Chem. Sci.*, 2013, **4**, 2463–2470.
27 J.-X. Hu, Y.-S. Meng, L. Zhao, H.-L. Zhu, L. Liu, Q. Liu, C.-Q. Jiao and T. Liu, *Chem. – Eur. J.*, 2017, **23**, 15930–15936.
28 F. F. Salomón, P. O. Abate and L. M. Baraldo, *Dalton Trans.*, 2024, **53**, 15083–15092.
29 S. E. Domínguez, M. V. Juarez, G. E. Pieslinger and L. M. Baraldo, *Eur. J. Inorg. Chem.*, 2022, **2022**, e202100843.
30 D. Aguila, Y. Prado, E. S. Koumousi, C. Mathoniere and R. Clerac, *Chem. Soc. Rev.*, 2016, **45**, 203–224.
31 S.-I. Ohkoshi and H. Tokoro, *Acc. Chem. Res.*, 2012, **45**, 1749–1758.
32 T. Shiga, N. Mihara and M. Nihei, *Coord. Chem. Rev.*, 2022, **472**, 214763.
33 P. Albores, L. D. Slep, L. S. Eberlin, Y. E. Corilo, M. N. Eberlin, G. Benitez, M. E. Vela, R. C. Salvarezza and L. M. Baraldo, *Inorg. Chem.*, 2009, **48**, 11226–11235.
34 C. Zeng, Q. D. Xu, X. L. Liu, Y. Y. Yang, S. M. Hu, X. T. Wu and T. L. Sheng, *Chem. – Eur. J.*, 2023, **29**, e202300433.
35 J.-H. Fu, Y. He, Y. Song, B.-C. Tan, X.-L. Liu, Y. Li, X.-T. Wu and T.-L. Sheng, *Cryst. Growth Des.*, 2024, **24**, 6218–6229.
36 S. D. Su, Y. H. Wen, X. T. Wu and T. L. Sheng, *Dalton Trans.*, 2022, **51**, 10047–10054.
37 S. D. Su, X. Q. Zhu, Y. H. Wen, X. T. Wu and T. L. Sheng, *Eur. J. Inorg. Chem.*, 2021, **2021**, 3474–3480.
38 S.-D. Su, X.-Q. Zhu, L.-T. Zhang, Y.-Y. Yang, Y.-H. Wen, X.-T. Wu, S.-Q. Yang and T.-L. Sheng, *Dalton Trans.*, 2019, **48**, 9303–9309.
39 T. L. Sheng, R. Appelt, V. Comte and H. Vahrenkamp, *Eur. J. Inorg. Chem.*, 2003, 3731–3737.
40 A. Vogler, A. H. Osman and H. Kunkely, *Inorg. Chem.*, 1987, **26**, 2337–2340.
41 C. A. Bignozzi, S. Roffia and F. Scandola, *J. Am. Chem. Soc.*, 1985, **107**, 1644–1651.
42 N. Y. Zhu and H. Vahrenkamp, *Angew. Chem., Int. Ed. Engl.*, 1994, **33**, 2090–2091.
43 N. Y. Zhu and H. Vahrenkamp, *Chem. Ber./Recl.*, 1997, **130**, 1241–1252.
44 S. E. Dominguez, G. E. Pieslinger, L. Sanchez-Merlinsky and L. M. Baraldo, *Dalton Trans.*, 2020, **49**, 4125–4135.
45 P. S. Oviedo, G. E. Pieslinger, A. Cadranel and L. M. Baraldo, *Dalton Trans.*, 2017, **46**, 15757–15768.
46 G. E. Pieslinger, B. M. Aramburu-Troselj, A. Cadranel and L. M. Baraldo, *Inorg. Chem.*, 2014, **53**, 8221–8229.
47 S.-H. Li, Y. Liu, Y.-Y. Yang, Y.-X. Zhang, Q.-D. Xu, S.-M. Hu, X.-T. Wu and T.-L. Sheng, *Polyhedron*, 2019, **173**, 114109.
48 S.-H. Li, Y.-Y. Yang, Y.-X. Zhang, X.-T. Wu and T.-L. Sheng, *Chin. J. Struct. Chem.*, 2021, **40**, 207–216.
49 X.-L. Liu, Y. Li, Q.-D. Xu, Z.-Q. Wei, X.-T. Wu and T.-L. Sheng, *New J. Chem.*, 2022, **46**, 7922–7927.
50 X. Ma, C.-S. Lin, H. Zhang, Y.-J. Lin, S.-M. Hu, T.-L. Sheng and X.-T. Wu, *Dalton Trans.*, 2013, **42**, 12452–12459.
51 L.-T. Zhang, X.-Q. Zhu, S.-M. Hu, Y.-X. Zhang, S.-D. Su, Y.-Y. Yang, X.-T. Wu and T.-L. Sheng, *Dalton Trans.*, 2019, **48**, 7809–7816.
52 L.-T. Zhang, X.-Q. Zhu, S.-D. Su, Y.-Y. Yang, S.-M. Hu, Y.-H. Wen, X.-T. Wu and T.-L. Sheng, *Cryst. Growth Des.*, 2018, **18**, 3674–3682.
53 R. Appelt and H. Vahrenkamp, *Inorg. Chim. Acta*, 2003, **350**, 387–398.
54 Z. N. Chen, R. Appelt and H. Vahrenkamp, *Inorg. Chim. Acta*, 2000, **309**, 65–71.
55 G. N. Richardson, U. Brand and H. Vahrenkamp, *Inorg. Chem.*, 1999, **38**, 3070–3079.
56 T. Sheng and H. Vahrenkamp, *Inorg. Chim. Acta*, 2004, **357**, 1739–1747.
57 T. L. Sheng and H. Vahrenkamp, *Eur. J. Inorg. Chem.*, 2004, 1198–1203.
58 N. Y. Zhu and H. Vahrenkamp, *J. Organomet. Chem.*, 1999, **573**, 67–72.
59 X.-L. Liu, Y. Li, Q.-D. Xu, Y.-Y. Yang, J.-H. Fu, X.-T. Wu and T.-L. Sheng, *Inorg. Chem.*, 2022, **61**, 17392–17401.
60 Y. Song, J.-H. Fu, B.-C. Tan, Q. Wang, L.-L. Jiang, X.-T. Wu and T.-L. Sheng, *Polyhedron*, 2023, **240**, 116446.
61 Q.-D. Xu, X. Ma, C. Zeng, S.-D. Su, S.-M. Hu, Y.-Y. Huang, X.-T. Wu and T.-L. Sheng, *Chem. – Eur. J.*, 2022, **28**, e202104486.

62 Q.-D. Xu, C. Zeng, S.-D. Su, Y. He, Y. Liu, S.-M. Hu, X.-T. Wu and T.-L. Sheng, *Dalton Trans.*, 2022, **51**, 13938–13948.
63 Q.-D. Xu, C. Zeng, S.-D. Su, Y.-Y. Yang, S.-M. Hu, T.-Y. Li, X.-T. Wu and T.-L. Sheng, *Dalton Trans.*, 2021, **50**, 6161–6169.
64 Q.-D. Xu, L.-T. Zhang, C. Zeng, Y.-Y. Yang, S.-D. Su, S.-M. Hu, X.-T. Wu and T.-L. Sheng, *Chem. – Eur. J.*, 2021, **27**, 11183–11194.
65 Y.-Y. Yang, X.-Q. Zhu, J.-P. Launay, C.-B. Hong, S.-D. Su, Y.-H. Wen, X.-T. Wu and T.-L. Sheng, *Angew. Chem., Int. Ed.*, 2021, **60**, 4804–4814.
66 Y.-Y. Yang, X.-Q. Zhu, Y. Wang, X.-T. Wu and T.-L. Sheng, *Inorg. Chem. Front.*, 2022, **9**, 4732–4740.
67 C. Zeng, Q.-D. Xu, X.-L. Liu, S.-M. Hu, X.-T. Wu and T.-L. Sheng, *Dalton Trans.*, 2023, **52**, 16858–16869.
68 X. Ma, C.-S. Lin, X.-Q. Zhu, S.-M. Hu, T.-L. Sheng and X.-T. Wu, *Angew. Chem., Int. Ed.*, 2017, **56**, 1605–1609.
69 T. Liu, Y.-J. Zhang, S. Kanegawa and O. Sato, *Angew. Chem., Int. Ed.*, 2010, **49**, 8645–8648.
70 H. Oshio, H. Onodera and T. Ito, *Chem. – Eur. J.*, 2003, **9**, 3946–3950.
71 M. Nihei, M. Ui, N. Hoshino and H. Oshio, *Inorg. Chem.*, 2008, **47**, 6106–6108.
72 T.-Y. Li, S.-D. Su, Y. He, X.-T. Wu and T.-L. Sheng, *Dalton Trans.*, 2024, **53**, 5010–5019.
73 T.-Y. Li, S.-D. Su, Y.-Y. Yang, Y. He, H. Liu, X.-T. Wu and T.-L. Sheng, *Cryst. Growth Des.*, 2023, **23**, 9075–9085.
74 S.-D. Su, Y.-H. Wen, X.-T. Wu and T.-L. Sheng, *Dalton Trans.*, 2022, **51**, 10047–10054.
75 S.-D. Su, X.-Q. Zhu, Y.-H. Wen, X.-T. Wu and T.-L. Sheng, *Eur. J. Inorg. Chem.*, 2021, **2021**, 3474–3480.
76 J.-X. Hu, L. Luo, X.-J. Lv, L. Liu, Q. Liu, Y.-K. Yang, C.-Y. Duan, Y. Luo and T. Liu, *Angew. Chem., Int. Ed.*, 2017, **56**, 7663–7668.
77 Y.-Y. Huang, Y. He, Y. Liu, J.-H. Fu, X.-L. Liu, X.-T. Wu and T.-L. Sheng, *Dalton Trans.*, 2024, **53**, 3777–3784.
78 Y.-Y. Huang, Y. He, Y.-Y. Yang, Y. Wang, X.-T. Wu and T.-L. Sheng, *Cryst. Growth Des.*, 2024, **24**, 3044–3054.